Science of the Total Environment 628–629 (2018) 1108–1120

Contents lists available at ScienceDirect

Science of the Total Environment

journal homepage: www.elsevier.com/locate/scitotenv

Storm induced estuarine turbidity maxima and controls on nutrient fluxes across river-estuary-coast continuum

Nengwang Chen [a,b,*], Michael D. Krom [c,d], Yinqi Wu [b], Dan Yu [b], Huasheng Hong [a,b]

[a] State Key Laboratory of Marine Environmental Science, Xiamen University, Xiamen, China
[b] Fujian Provincial Key Laboratory for Coastal Ecology and Environmental Studies, College of the Environment and Ecology, Xiamen University, Xiamen, China
[c] School of Marine Sciences, University of Haifa, Haifa, Israel
[d] School of Earth and Environment, University of Leeds, Leeds, UK

HIGHLIGHTS

- Storm induced estuary turbidity maxima and controls on nutrient flux.
- Relatively more dissolved nutrients but less particulate phosphorus delivered to coast.
- The estuary-bay ecosystem became potentially P limited following storms.

GRAPHICAL ABSTRACT

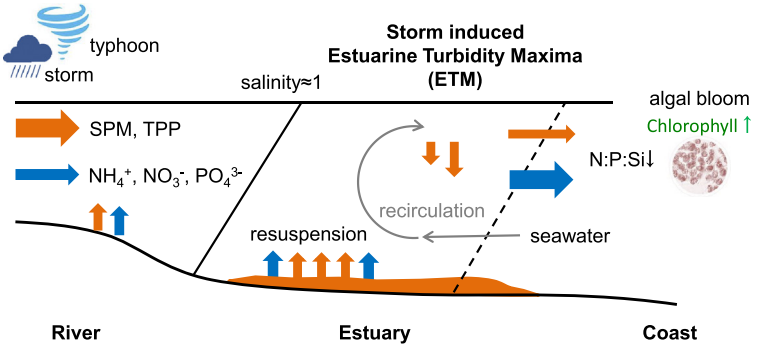

ARTICLE INFO

Article history:
Received 24 November 2017
Received in revised form 28 January 2018
Accepted 6 February 2018
Available online 20 February 2018

Editor: Ouyang Wei

Keywords:
Nutrient
Storm
Estuarine turbidity maxima
Eutrophication
Climate change
Jiulong River Estuary

ABSTRACT

Climate change is likely to increase the frequency and intensity of tropical storms. However, the impacts of major storms on nutrient cycling processes in the river-estuary-coast continuum are poorly understood. Continuous observations were made at lower river stations and on a transect down the Jiulong River Estuary in south east China for three storms in 2013–2014. There were major increases in both dissolved nutrients and suspended particulate matter (SPM) brought down the river during storms. Strong Estuarine Turbidity Maxima (ETM) were observed during major storms and were the result of SPM brought down rivers augmented by sediment scoured within the Upper Estuary (salinity = 0 psu) and possibly also from behind the dikes opened for flood control. There were major increases in dissolved nutrients (nitrate, ammonium and phosphate) in the Upper Estuary particularly during major Storms C (July 2013) and D (May 2014). These increases were probably due to river inflows with surrounding runoff, pore water supply and nutrients desorbed from scoured sediment. During major Storm D there were greater nutrient fluxes through the estuary-coast interface compared to the nutrients supplied through the river-estuary interface while the opposite pattern was observed during normal flow. The increased supply of ammonium and phosphate to the coastal region caused increased chlorophyll *a* once the light inhibiting SPM had been removed from the water column. This is likely to increase the potential of eutrophication. Storm induced increases in N:P:Si supplied from the estuary to the coastal region increased the degree of P limitation.

© 2018 Elsevier B.V. All rights reserved.

* Corresponding author at: College of the Environment and Ecology, Xiamen University, Xiamen 361102, PR China.
E-mail address: nwchen@xmu.edu.cn (N. Chen).

https://doi.org/10.1016/j.scitotenv.2018.02.060
0048-9697/© 2018 Elsevier B.V. All rights reserved.

1. Introduction

Nutrients are supplied to the ocean from land, where they are produced principally by anthropogenic activities (agriculture, domestic and industrial wastewater discharges) with natural weathering processes being less important (Mackenzie et al., 2002). Rivers and wastewater treatment plants discharge their nutrient loads into estuaries, which act as gatekeepers to the delivery of nitrogen (N) and phosphorus (P) to the ocean, particularly as a result of processes in the Estuarine Turbidity Maxima (ETM aka Turbidity Maximum Zone). A recent review on nutrients in estuaries highlighted the potential impact of climate change (Statham, 2012). Climate change is likely to increase the frequency and intensity of extreme climatic events (e.g., tropical storms, hurricanes, etc.) (Peierls et al., 2003; Qin et al., 2007; Statham, 2012). Major storms often cause much larger export of particles and nutrients from the watershed and faster transport down river and into the estuary than under normal hydrological condition (Chen et al., 2012; Chen et al., 2015; Paerl and Peierls, 2008; Rabalais et al., 2009). A single storm event can represent a hydrologic "hot" moment for transport or delivery of the majority of the annual nutrient load (McKee et al., 2000; Vidon et al., 2010). At the same time, point and nonpoint source pollution of macronutrients from urbanization and agriculture are increasing globally. While major investment has been made in many developed countries to reduce nutrient fluxes into rivers and coastal zones by improved sewage treatment, major storms can often overwhelm and/or temporarily bypass such systems (Lee et al., 2002). Global climate change and increased nutrient loading particularly during storm flows intensify eutrophication and cause more frequent or severe hypoxia in estuarine and coastal waters (Paerl, 2006; Rabalais et al., 2010; Rabalais et al., 2009; Statham, 2012).

Estuaries are key locations that modify the flux and nature of nutrient species from the river to the coastal zone. The ETM is considered an especially important location for affecting such nutrient cycling. Under normal flow conditions, it is the location where river-borne suspended load can be flocculated and mixed with estuarine sediment resuspended by tidal processes into the water column (Schubel, 1968), including any accumulated pore waters and chemically reactive mineral species that have been added since the sediment was deposited (Couceiro et al., 2013; Mortimer et al., 1999; Wengrove et al., 2015). The formation of the ETM typically occurs around a salinity of 1 psu, e.g. St. Lawrence (Gobeil et al., 1981), Delaware (Biggs et al., 1983), Gironde (Herman and Heip, 1999). Storms are periods of high particulate matter being brought down the river and times when there is considerable scour of sediments, which have been deposited possibly months to years previously depending on the magnitude and frequency of storm events. The storm generated ETM identified in this study thus represents potentially important locations for major changes in nutrient cycling compared with normal flow conditions. The longer the period since the last resuspension, the greater will be the flux of these additional chemical species into the water column as organic matter in the sediment is broken down by bacterial respiration (Abril et al., 1999).

Several recent studies based on satellite images and monitoring data have investigated the impact of large river discharge or floods on coastal ecosystems. For example, Yangtze River floods with major terrigenous nutrient input enhance phytoplankton biomass in the coastal ocean (Gong et al., 2011; Wang et al., 2015). Light conditions, water temperature, nutrient availability, water residence time are known as important factors controlling aquatic photosynthesis and growth of phytoplankton (Bledsoe et al., 2004; Dix et al., 2013; Falkowski and Raven, 2013). Strong wind and surface water currents caused by storms can result in less favorable conditions for phytoplankton growth. However, due to a lack of proper observation techniques and operational difficulties under extreme weather condition, comparatively few studies have been carried out on storm-induced nutrient biogeochemical processes through estuaries and into coastal waters (Herbeck et al., 2011; Zhang et al., 2009; Zhou et al., 2012). Little is known about the relative differences in the responses of nutrients (particulate and dissolved; organic and inorganic) to storms varying in rainfall intensity. Furthermore, a large knowledge gap exists in the linkage between biogeochemical processes and the ecological response which results in coastal eutrophication problems (Cloern, 2001).

The key question we seek to address is how do major storm events influence nutrient export, transport and transformation from the watershed via the estuary to the coast. Here we used opportunistic observational studies and successfully captured the storm-driven runoff encompassing river sites and estuary-bay stations in a nutrient-rich river estuary in southeast China. Continuous observations were carried out during three major storms that occurred in 2013–2014. The objectives of this study were: (a) to investigate the storm-driven exports of macronutrients (N, P, Si) from the river to the estuary and bay; (b) to identify and quantify the storm induced ETM and investigate its source and involvement in altering nutrient fluxes through the estuary; and (c) to quantify changes in biogeochemical behavior in estuary and seaward fluxes following major storm events including the magnitude of changes in stoichiometric ratios.

2. Methodology

2.1. Study area

The Jiulong River in southeast China has a drainage area of 14,740 km^2. The catchment has a population of over 3.5 million and is mainly mixed agriculture with several urban areas (Fig. 1). The climate is subtropical with an annual rainfall of 1400–1800 mm, 75% of which occurs between April and September when typhoons/tropical cyclones and major storms commonly occur. The Jiulong River Estuary receives a total annual mean runoff (1.24×10^{10} m^3 y^{-1}) from the North River (66%) and the West River (34%). The South river is another smaller tributary, which discharges into the middle estuary. There are six dam reservoirs (primarily for hydropower generation and flood control) in the main stem of the North River, while in the West River most dams (which are relatively small) are located in tributaries rather than in the main stem. In addition, there is a dike in each river immediately above the location where in normal flow conditions there is an increase in water salinity (i.e. the estuary). These result in a small reservoir in each of the main tributaries downstream of the last river sampling site. These dikes are opened during high flow periods for flood control. Jiulong River Estuary is a semi-enclosed macrotidal estuary with a tidal range of 2.7–4 m, an open water area of 100 km^2 and a depth of 3–16 m. The river runoff mainly flows into the south channel of estuary and Xiamen Bay (Guo et al., 2011). The average flushing time of estuary during normal flow has been estimated as 2–3 days (Cao et al., 2005).

In this study, we define the Upper Estuary as the region of the estuary with zero salinity during the storms, which starts at A4 (Fig. 1), the location where the first sample of brackish water is usually found at flood tide. The Middle Estuary is the region from <0.1 psu to 5 psu, the first samples of brackish water during the storms (Fig. 2). The Lower Estuary is the region of brackish water >5 psu as far as Xiamen Bay.

2.2. Sampling campaign and lab analysis

A rain storm is meteorologically defined as daily rainfall greater than 50 mm and results in drastically increased river flow. In this study, the date of sampling was opportunistic and was based on the storm driven changes in river discharge (see SI for description of the detailed reasons for the sampling dates chosen). The Stormflow (pulse) event was defined as starting when hourly discharge more than doubled, and was considered to end when flow fell below double the previous baseflow. The normal flow condition was when riverflow had been reduced close to the previous baseflow and the 0–1 psu boundary was adjacent to station A4 (Fig. 2 and Fig. S1). Previous studies examined riverine P export during Storms A, B and C (Chen et al., 2015), while this study

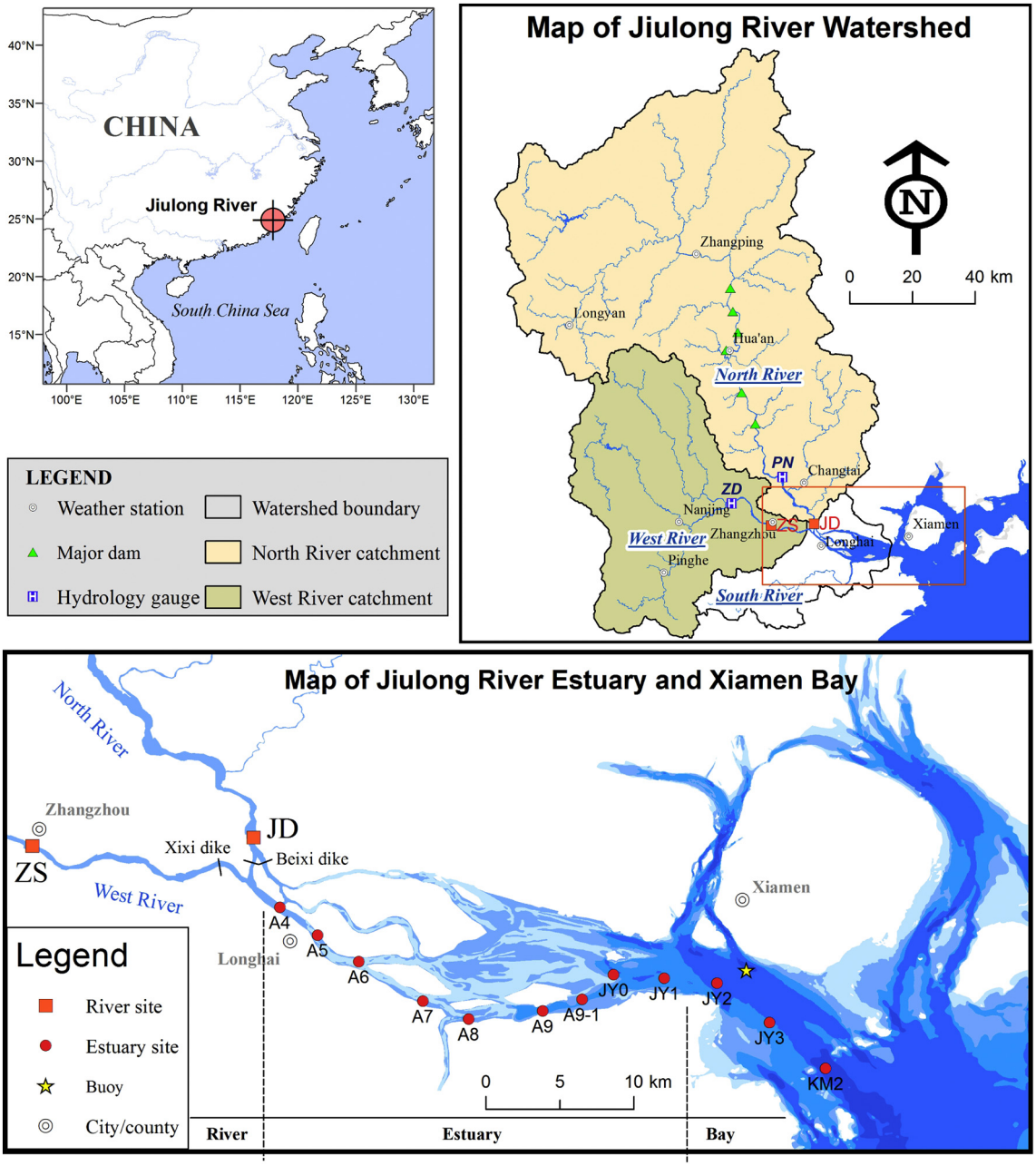

Fig. 1. Map of study area showing sampling sites (red circle) along the Jiulong river-estuary gradient. Jiangdong (JD) at the lower North River and Zhongshan (ZS) at the lower West River were selected as the fixed sampling sites for continuous measurements during storm periods. The Upper Estuary was defined as the part of the 'normal' estuary, which was occupied by freshwater as a result of the storm. During major storm events, the freshwater-salinity boundary may move to station A9.

focused on macro nutrients (N, P, Si) delivery and cycling through the estuary in the same Storm C, and two subsequent Storms D and E.

To understand how storm runoff influenced nutrient export and transport, observations were conducted in a series of stations from station A4 above Longhai, downstream along a river-estuary-bay transect (A4-KM2; Fig. 1). Samples were also taken at two lower river sites (JD, ZS) except during Storm C when there was no sampling at ZS in the lower West River. A set of cruises along the Jiulong River Estuary were carried out to sample the surface (1 m) water with or without the effects of stormflow. It was not possible for practical reasons to measure the vertical salinity gradient (or nutrient concentrations with depth) during this storm sampling. However we would expect the water in the Upper Estuary, which has a salinity of <0.1 psu, to be well mixed vertically because of the relatively shallow depth and because previous measurements in the Upper Estuary during normal flow show a well-mixed water column. Nutrient measurements in the Lower Estuary during the storms show conservative behavior. As a result the calculations of the nutrient fluxes through the river-estuary interface (REI) and estuary-coast interface (ECI) calculated below are considered to be robust.

Measurements taken 1–2 days after peak discharge of storms were regarded as the "storm-affected" conditions (Fig. S1). Given the uncertainty of weather forecast and practical reasons, pre-storm measurements were measured only for Storm E. Measurements conducted 10 days after peak discharge of Storm C, and 22 days after Storm D were considered to represent normal conditions as the river hydrograph had returned to normal summer flow and salinity had returned from ~0–10 psu to a typical range of 0–30 psu in the studied

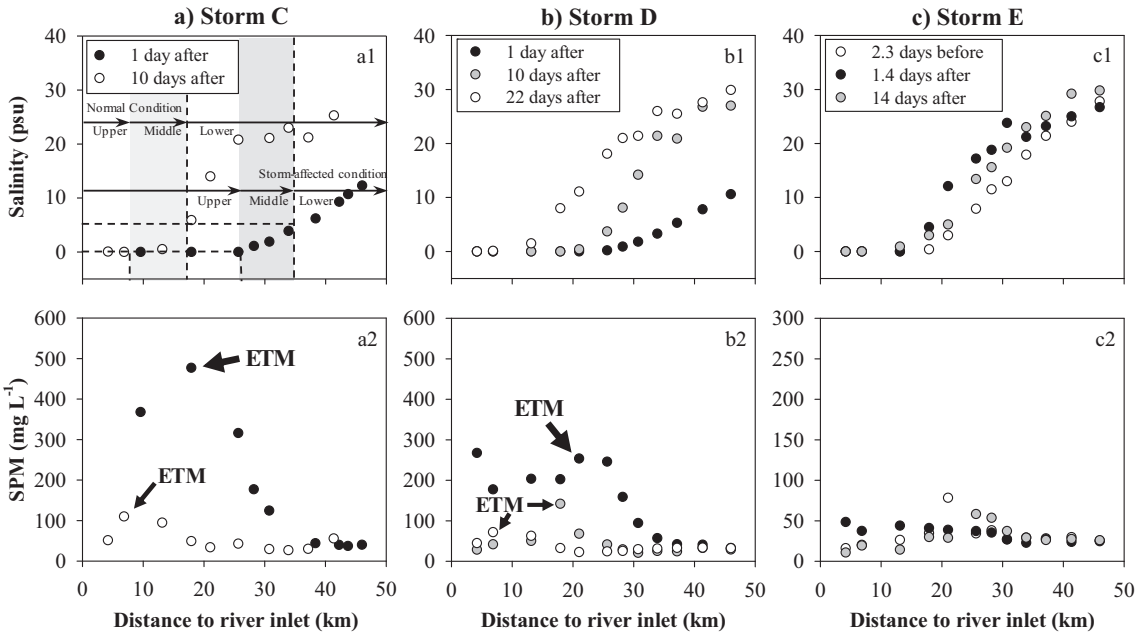

Fig. 2. Spatial variation of salinity along river-estuary-bay gradient by storm events. Measured at stations A4-KM2. The zero location is JD (refer to Fig. 1). Measurements 1–1.4 days after peak discharge of storms (C, D, E) were regarded as the 'storm-affected' conditions (solid circles). Measurements conducted 10 days after peak discharge of Storm C, and 22 days after Storm D and 2.3 days before Storm E were considered to represent "normal" conditions (blank circles) as the river hydrograph had returned to summer normal flow. Arrow shows major storm induced a stronger ETM. The Upper Estuary is defined as the region of the estuary with zero salinity starting at A4. The Middle Estuary is the region from <0.1 psu to 5 psu. The Lower Estuary is the region of brackish water >5 psu as far as Xiamen Bay.

sites. See Supplementary Information for detailed justification of the time of sampling.

The salinity of each discrete sample was measured in the field using a portable water quality Meter (WTW Multi 3430, Germany). A buoy (LOBO) with a water quality probe (YSI® 6600, USA) was deployed in Xiamen Bay (1 m depth) providing long-term observation of chlorophyll *a*, salinity, water temperature, turbidity and nitrate during Storm C. The fresh water and nutrient loading around the buoy were mainly affected by Jiulong River. Underway measurement of water quality using another probe (YSI® 6600, USA) was performed 10 days after Storm C. At the two river sites, we used an automatic water sampler (Teledyne ISCO 6712, USA) to collect storm runoff (1 m depth) at an interval of 2 h during the flood periods. A total of 12 water samples per day were stored in a container with ice for cooling before delivery to the laboratory at Xiamen University.

After filtration through a GF/F filter, all water samples and filters were frozen at −20 °C before analysis of dissolved and particulate nutrients. Filtered water was analyzed by segmented flow automated colorimetry using the manufacturer's standard procedures (San++ analyser, The Netherlands) for the sum of nitrate and minor nitrite (called NO_3-N here), ammonium (NH_4-N), total dissolved N (TDN), soluble reactive phosphorus (SRP), total dissolved phosphorus (TDP) and dissolved silica (DSi). Samples for TDN and TDP were oxidized to nitrate and phosphate by 4% alkaline potassium persulfate before measurement. Suspended particulate matter (SPM) was determined gravimetrically as the difference between the pre-weighed and filtered GF/F filters after oven-drying to constant weight. Subsequently, the oven-dried filters were analyzed for total particulate phosphorus (TPP) after being combusted in a muffle furnace (550 °C for 1.5 h) (to convert organic P to inorganic P), subsequently extracted with 1 M HCl and analyzed as phosphate (SRP) as stated above. Dissolved inorganic nitrogen (DIN) was summed from NO_3-N and NH_4-N. Dissolved organic nitrogen (DON) and dissolved organic phosphorus (DOP) were obtained by subtracting DIN from TDN, and SRP from TDP, respectively. The precision for nutrient analysis was estimated by repeated determinations of 10% of the samples and the relative error was 2%–5%. Commercial standard reference materials were used to check the instrument performance.

2.3. Auxiliary data collection and data analysis

Hourly rainfall records for eight weather stations in the catchment and wind at Xiamen were obtained from Weather China (http://www.weather.com.cn/). Hourly river discharge was obtained from hydrological stations (PN in the North River and ZD in the West River; Fig. 1).

In order to examine the impact of major storms on nutrient dynamics and potential estuarine processes (e.g., ETM associated), the flow-weighted mean concentrations (FMC) were calculated from the sum of the total substance flux (kg s^{-1}) at river sites (JD and ZS) divided by the combined water flow (L s^{-1}) at those sites during Storm D and E. The river discharge recorded at hydrological stations (PN and ZD) was extrapolated to river sites using the ratios of the drainage area between them. We also adjusted the timing, so it represents the 2 h signal at JD and ZS. Time series fluxes were then calculated as products of the concentration and discharge. All measurements along the salinity gradient were used to explore if the ETM and associated nutrient behavior (addition or removal) changed with storms. Non-conservative behavior of nutrient can be interpreted as deviations from conservative mixing line of marine and freshwater end-member (Officer, 1979).

In order to quantify the amount of nutrients reaching the coastal zone following storms, the nutrient fluxes across the river-estuary interface (REI) and estuary-coast interface (ECI) were compared. REI flux (ton d^{-1}) was directly calculated as the concentration of the uppermost freshwater site (salinity<0.1 psu) in the Upper Estuary and the river water flux (m^3 d^{-1}) of the sampling day. This calculation includes nutrients supplied from the river catchment plus any changes caused by possible resuspension of sediment in the reservoirs below JD/ZS when the sluice gates are opened during storms.

The ECI flux represents the nutrient export from the Lower Estuary to coastal water at interface with salinity = 30 psu and was estimated using the procedure described by Officer (1979). A better regression line fit was made to the observed concentration and salinity values in

the high salinity region in the lower reaches of the estuary (typically conservative mixing). This regression line was then extrapolated back to salinity = 0 to give a concentration value, C_0^*. Total river water flow ($m^3\ d^{-1}$) on the sampling day was multiplied by C_0^* to obtain the ECI fluxes (ton d^{-1}). The fraction of each chemical species making up the total dissolved N and total P fluxing through the two boundaries (REI and ECI) were calculated. We developed linear regression curves (concentration versus salinity) for N and P species in Storm D and E (Storm C was not considered since measurements in the West River were not available). SRP at higher salinity (>15 psu) was not available for the measurement 1 day after Storm D because of the strong river plume. We assumed a linear relationship still existed in the high salinity region. The SRP concentration varied little at the seawater end-member in the short term. Then we combined the SRP concentrations at salinity around 30 psu measured in the other two cruises (10 and 20 days after storm D) and storm-affected SRP data (salinity >6 psu) to make a linear interpolation to obtain C_0^*.

3. Results

3.1. Meteorological and hydrological condition of studied storm events

Three storm events, which occurred on July 13–14, 2013 (Storm C, caused by Typhoon Soulik), May 21–23, 2014 (Storm D, the first major storm of the year) and July 23–24, 2014 (Storm E) were studied and their characteristics were compared (Table 1). Storm C had a shorter duration but a higher rainfall intensity (132 mm d^{-1}) and a larger peak discharge (3070 $m^3\ s^{-1}$) compared with Storm D and E. During Storm D, the North River catchment had less rainfall intensity (47 mm d^{-1}) and longer duration, than the West River catchment (77 mm d^{-1}). Peak discharge (2440 $m^3\ s^{-1}$ of the North river, 1520 $m^3\ s^{-1}$ of the West River) during Storm D was the largest recorded in 2014. For Storm E, the rainfall intensity and runoff were lower. For Storm D and Storm E, both runoff coefficient (=runoff/rainfall) and rainfall intensity were greater in the West River than in the North River. Storm D had the largest runoff coefficient (0.36 for the North River and 0.57 for the West River), followed by Storm C (0.26 for the North River) and Storm E (0.12 for the North River and 0.16 for the West River). Antecedent precipitation index (API) indicated that runoff was influenced by soil antecedent moisture conditions (Perrone and Madramootoo, 1998). The typical delay of the peak flow rate at the two gauging stations (PN, ZD) following the maximum rainfall was about 18–22 h. An exception to that was the quicker response of runoff to rainfall (10 h lag) that was found in the West River during Storm E, because the rainfall was concentrated in the lower river catchment for that storm. In the estuary area (Xiamen), the recorded wind speed during most cruises was <3.4 m s^{-1}. A higher wind speed of 5.5–10.8 m s^{-1} was recorded two days before Storm C and 10 days after Storm D, which is far below typhoon level (>32.6 m s^{-1}) as our studied sites were 150–200 km away from the typhoon center. Under this climate condition, wave height would be less than 0.3 m in most cruises but might reach 1–2 m when wind speed increased. The wave height was not measured in the JRE and Xiamen Bay but was visually estimated as less than 0.5 m even during 'storm-affected' cruises.

3.2. Riverine nutrients in storm runoff

The flow-weighted mean concentrations (FMC) based on time series measurements at two river sites (JD, ZS) during Storm D and E showed changes in river nutrient concentration during storm runoff (Table 2). Details of changes in the nutrient and SPM concentrations and fluxes with discharge are given in the Supplementary Information (Fig. S2). As the product of concentration and discharge, instantaneous nutrient fluxes varied with time and between storms. In general, the West river contributed a larger flux of NH_4-N, NO_3-N and SRP than the North River.

3.3. Changes in estuarine salinity and SPM under storm-affected conditions

The salinity along the river-estuary transects changed as a result of the storm events (Fig. 2). The fresh-saline water front (salinity 0–1 psu) moved at least 10 km downstream after Storm C and D while changing little in Storm E sampled 1.4 days after the storm. Both the Upper and Middle Estuary have high SPM during major storms and are the region of the storm induced ETM (Fig. 2).

In detail the total salinity range of the estuarine water sampled (A4-KM2) was reduced, particularly for major Storm C and D compared with normal conditions (Fig. 2). Salinity measured at station KM2 (as seawater end-member) decreased from around 30 psu (a typical value under normal condition) to 12.3 psu one day after Storm C, and to 10.6 psu one day after Storm D. Particulate matter (SPM and TPP) showed a marked increase during the major storms (Fig. 2 and Fig. S3). Storm-affected SPM in the Upper Estuary reached up to 477 mg L^{-1} in Storm C, and to 268 mg L^{-1} in Storm D, 2–6 times higher than that under normal condition (i.e., <100 mg L^{-1}), resulting in a strong Estuarine Turbidity Maximum (ETM). Location of the ETM also moved downward following major Storms C and D (Fig. 2). Peak values of TPP showed a similar trend as SPM, increasing from less than 5μmol L^{-1} under normal conditions to 12.0 μmol L^{-1} in Storm C and 8.3 μmol L^{-1} in Storm D. In Storm E, less change in SPM (40 to 50 mg L^{-1}) and TPP (an increase of ~1 μmol L^{-1}) were found between the sampling prior to the storm and sampling 1.4 days after the storm. Moreover, storm-affected

Table 1
Characteristics of rainfall and discharge for the three studied storm events.

Storm Event	Starting Date	River	Rainfall duration (h)	Mean rainfall (mm)	Rainfall intensity (mm d^{-1})	Stormflow duration (h)	Mean discharge ($m^3\ s^{-1}$)	Peak discharge ($m^3\ s^{-1}$)	Baseflow ($m^3\ s^{-1}$)	Peak delay (h)	Cumulative runoff (mm)	Runoff coefficient	API (mm)
C	7/13/2013	North	26	142.9	131.9	53	1682	3070	276	18	37.5	0.26	8.76 (I)
D	5/21/2014	North	51	100.3	47.2	59	1514	2440	343	21	36.6	0.36	76.90 (III)
	5/22/2014	West	22	70.8	77.2	55	679	1520	175	22	40.0	0.57	81.26 (III)
E	7/23/2014	North	40	76.1	45.7	53	375	650	146	20	9.0	0.12	1.42 (I)
	7/23/2014	West	36	113.9	75.9	53	328	579	98	10	18.7	0.16	7.28 (I)

Note. Mean rainfall was calculated using recorded hourly rainfall from four weather stations (Longyan, Zhangping, Hua'an and Changtai in the North Jiulong River and Longhai, Pinghe, Nanjing and Zhangzhou in the West Jiulong River). Stormflow (pulse) was defined as starting when discharge more than doubled and was considered to end when flow fell below double the previous baseflow. Baseflow was defined as the period of relatively steady flow prior to a hydrograph pulse. Peak delay is the time between the maximum rainfall in catchment and the peak water flow past stations Punan (PN) and Zhengdian (ZD) (Fig. 1). Cumulative runoff was calculated as total water mass divided by catchment area. Runoff coefficient was the ratio of cumulative runoff to rainfall. Antecedent precipitation index (API) = $\sum k^i P_i$, where P_i are precipitation 1, 2, …, i ($i = 14$) days prior to the event and k is a constant ($k = 0.85$).Three soil antecedent moisture conditions were classified according to API value. Condition I (dry): 0 ≤ API ≤ 15 mm; Condition II (average): 15 ≤ API ≤ 30 mm; Condition III (wet): API > 30 mm. API was adapted from Perrone and Madramootoo (1998).

Table 2
Comparison of the calculated net concentrations of parameters delivered from the Rivers and the concentrations of those parameters in the Upper Estuary and Middle Estuary under storm-affected conditions.

Storm event	Location*	NO_3-N ($\mu mol\ L^{-1}$)	NH_4-N ($\mu mol\ L^{-1}$)	SRP ($\mu mol\ L^{-1}$)	TPP ($\mu mol\ L^{-1}$)	DSi ($\mu mol\ L^{-1}$)	SPM ($mg\ L^{-1}$)
C	River (JD)	140.6 ± 5.3	20.9 ± 9.5	1.6 ± 0.2	13.9 ± 3.3	180.5 ± 6.4	680.0 ± 108.1
(July 2013)	Upper Estuary (0 psu)	231.6 ± 25.4	111.8 ± 1.0	5.0 ± 0.4	10.8 ± 1.6	195.0 ± 4.0	422.5 ± 77.1
	Middle Estuary (0.1–5 psu)	158.4 ± 6.0	105.3 ± 20.6	2.8 ± 0.2	5.9 ± 1.9	173.5 ± 8.5	180.3 ± 95.6
	Change from River through Upper Estuary	Added	Added	Added	Removed	Minor change	Removed
D	River (FMC)	267.8 ± 38.2	46.0 ± 4.6	2.9 ± 0.4	12.7 ± 5.1	289.5 ± 25.2	353.5 ± 108.6
(May 2014)	Upper Estuary (0 psu)	358.2 ± 37.0	72.1 ± 7.7	3.8 ± 0.4	6.5 ± 0.4	273.5 ± 30.7	212.8 ± 38.4
	Middle Estuary (0.1–5 psu)	310.0 ± 22.9	72.2 ± 2.0	2.8 ± 0.1	5.3 ± 2.5	352.8 ± 14.1	162.1 ± 88.0
	Change from River through Upper Estuary	Added	Added	Added	Removed	Minor change	Removed
E	River (FMC)	171.8 ± 8.8	70.6 ± 9.5	3.2 ± 0.7	3.0 ± 0.6	263.6 ± 7.5	45.3 ± 13.4
(July 2014)	Upper Estuary (0 psu)	219.1 ± 14.6	93.5 ± 8.9	5.2 ± 0.4	2.4 ± 0.5	253.6 ± 0.2	43.0 ± 7.8
	Middle Estuary (0.1–5 psu)	194.0 ± 14.4	117.1 ± 5.1	4.9 ± 0.0	1.9 ± 0.4	247.0 ± 15.2	42.5 ± 2.1
	Change from River through Upper Estuary	Added	Added	Added	Removed	Minor change	Removed

Note. Data were present as mean ± standard deviation. River (JD) indicating mean concentrations of continuous measurement at JD (North Jiulong River) on 14 July 2013 (8:00–24:00, sample number = 9) was used for simple comparison since ZS (West River) was not measured in Storm C. River (FMC) indicates mean flow-weighted mean concentrations which represent net concentrations of parameters delivered from the two rivers (Data from Fig. S2); Upper Estuary (0 psu) indicates mean value of measurements with salinity = 0. Middle Estuary (0.1–5 psu) is the mean value of measurements with salinity of 0.1–5 psu; Change was determined based on the difference between measurements of concentrations brought down the river and those found in the Upper Estuary. The location of the ETM is the Upper and Middle Estuary (Data from estuary cruises and comparison with normal data; Fig. 2).
Bold indicates difference at significance level a=0.05.

concentrations of SPM and TPP declined sharply in the Middle Estuary and approached the level of normal condition in the Lower Estuary (salinity >5 psu).

3.4. Changes in estuarine nutrient concentrations under storm-affected conditions

Nutrient-salinity relationships changed under storm-affected conditions compared with those under normal conditions (Fig. 3). There was a strong addition of NH_4-N in the Upper and Middle Estuary (low salinity and high SPM) area soon after all storms compared with low concentrations 10 days after Storm C and 22 days after Storm D. NH_4-N was generally more variable than other nutrient species even in high salinity water where it was usually conservative under normal condition. The NH_4-N-salinity relationship was variable in Storm E, though the concentration was higher throughout the estuary compared with the pre-storm values. For the measurements one day after Storm C and D, SRP concentrations decreased dramatically in the Upper Estuary then remained constant at ~2.5 $\mu mol\ L^{-1}$ and even slightly increased with salinity in the Middle Estuary. In Storm E, SRP showed typically conservative mixing over the entire salinity range reaching ~1.5 $\mu mol\ L^{-1}$ at high salinity (coastal) values. The behavior 1.4 days after the storm E and under normal conditions was similar. For DSi there was simple conservative mixing over the entire salinity range for Storm C and E, while there was a small increase in DSi at low salinity in the Middle Estuary in Storm D.

The mean concentrations in the River (storm runoff), the Upper Estuary, which is within the zone of increasing salinity under normal flow conditions (Fig. 2) and the Middle Estuary where salinity begins to increase during storm flow were compared in Table 2. NO_3-N showed a large increase in concentration in the Upper Estuary compared with the river in Storm C and D followed by conservative mixing at higher salinities. Although the Upper Estuary has the highest SPM in the estuary compared with values downstream and is the location of the start of the storm induced ETM, the values of SPM and TPP are lower than those measured in the river as it flows past JD and ZS. There was a major decrease in SPM and TPP for all storms between the river and the Upper Estuary and between the Upper Estuary and the Middle Estuary for Storm C and D while for Storm E the change was small. By contrast for all dissolved nutrients (NO_3-N, NH_4-N and SRP) there were higher concentrations in the Upper Estuary compared to the River values, implying an additional source of dissolved nutrients. There was then a decrease in nutrients into the Middle Estuary for NO_3-N and SRP (all storms) and NH_4-N for Storm C though there was no change in NH_4-N for Storm D and a small increase in NH_4-N for Storm E. DSi changed little although there was a slight increase in Storm C and a small decrease in Storm D and E between the river and the Upper Estuary and an increase in Storm D and small decreases in Storm C and E between the Upper and Middle Estuary.

As a combined result of changing forms of the estuarine nutrients, the mean DIN:SRP ratios (storm-affected) increased to 79 in Storm C and to 112 in Storm D but varied little in Storm E, compared with normal values of 29–68 (Fig. 4). The mean DSi:DIN ratios of 1.1–1.8 (normal) mostly decreased to 0.7–0.9 (storm-affected) as DIN increased much more. In general, the N:P:Si ratios has less spatial variation under storm-affected relative to normal condition.

3.5. Changes in nutrient fluxes across river-estuary-coast interfaces

Storms resulted in large increases in freshwater inflows and nutrient loading to the estuary and from the estuary to the coast. The river-estuary fluxes and estuary-coast fluxes of each nutrient species were compared between normal and storm-affected condition for Storms D and E (Fig. 5). Fluxes of TDN (=NO_3 − N + NH_4 − N + DON) and TP (=TPP + SRP + DOP) in Storm D increased 2.5–4.5 folds compared with those under normal condition. These fluxes were also slightly increased in Storm E. Relative contribution of inorganic nitrogen increased during storms while organic nitrogen (from normal 25%–57% to storm-affected 2%–23%) decreased. The fluxes of TDN (and all N species) were much greater during the major storm (Storm D) than under normal conditions with the TDN fluxes (storm-affected) through ECI generally greater than REI fluxes, which is the opposite to that under normal condition where TDN fluxes through ECI was less than REI fluxes. By contrast in the smaller Storm E, TDN fluxes were similar to those under normal conditions.

The TP fluxes through these boundaries were higher for both REI and ECI for both Storm D and Storm E compared with normal conditions. The SRP fluxes through REI were lower (13 ton d^{-1} in Storm D, 7.7 ton d^{-1} in Storm E) than ECI (16 ton d^{-1} in Storm D, 10 ton d^{-1} in Storm E) under storm-affected condition while SRP fluxes through REI were higher than that through ECI under normal condition (Fig. 5). By contrast TPP fluxes through REI during Storm D were far greater than that through ECI, and relative contribution of TPP increased from 15% to 49% while SRP decreased from 49% to 17%.

Fluxes of DSi through both REI and ECI increased by a factor of 3.1 in Storm D and by 1.5 in Storm E compared with those under normal condition (Fig. 5). There was a minor increase of DSi (<10%) from REI to ECI under both normal and storm-effected condition in Storm D and E.

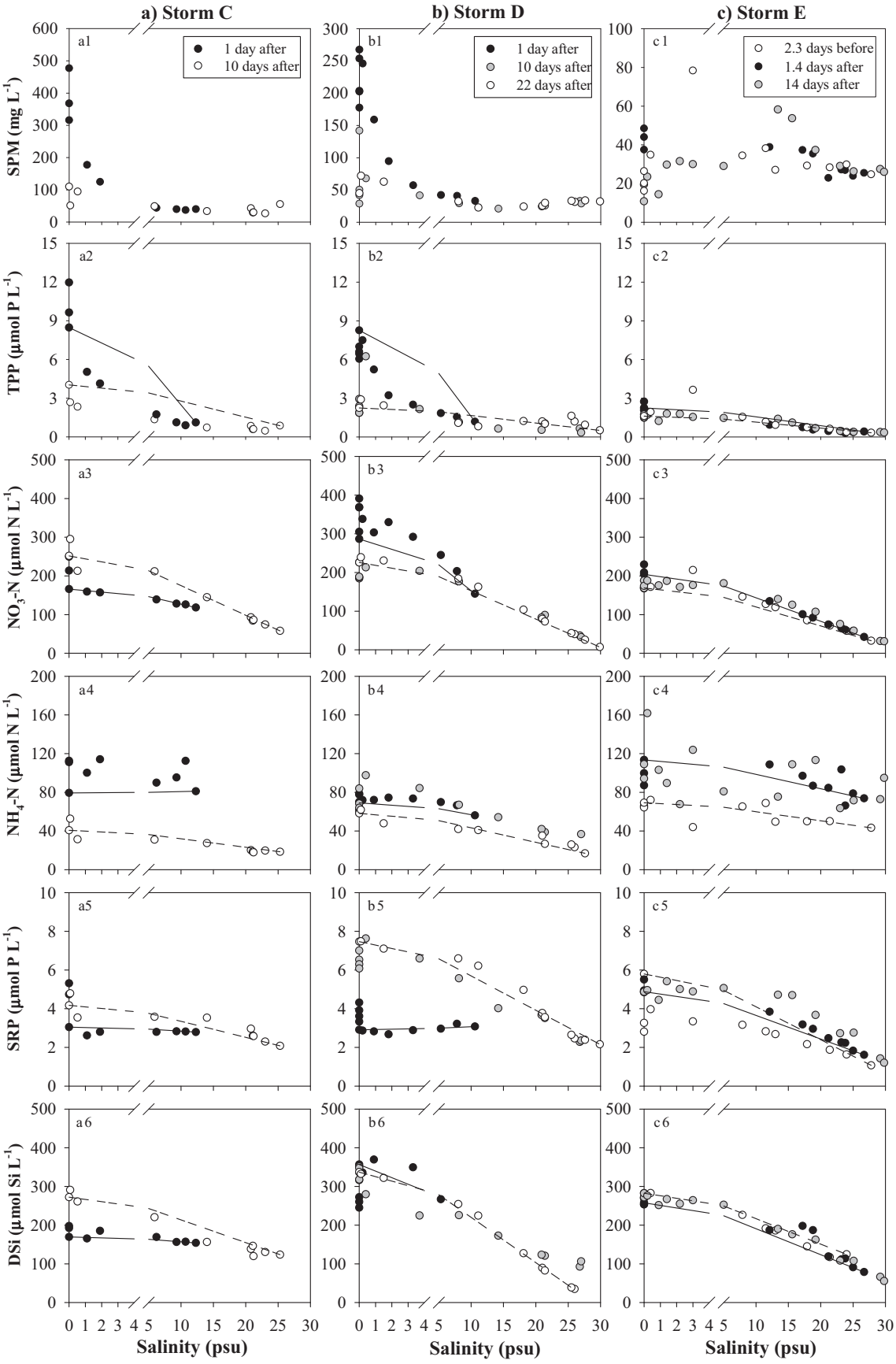

Fig. 3. Relationships between the measured parameters and salinity down the estuary showing both storm-affected data and data collected under normal conditions. Measurements 1–1.4 days after peak discharge of storms (C, D, E) were regarded as the 'storm-affected' conditions (solid circles). Measurements conducted 10 days after peak discharge of Storm C, and 22 days after Storm D and 2.3 days before Storm E were considered to represent 'normal' conditions (blank circles) as the river hydrograph had returned to summer normal flow. Solid lines and dash lines represent conservative mixing lines during 'storm-affected' and 'normal' conditions, respectively.

3.6. Time series of salinity, nitrate and chlorophyll a in Xiamen bay during major storm

In-situ observations by LOBO buoy showed hourly variation of salinity, water temperature, turbidity, nitrate, and chlorophyll *a* in Xiamen bay around the period of a series of rainfall events caused by typhoon and tropical cyclones in summer 2013 (Fig. 6). One day after typhoon Soulik landed (i.e., Storm C), salinity range declined suddenly from 21 to 30 psu to less than 10 psu while nitrate concentration increased from approximately 60 μmol L^{-1} to 120 μmol L^{-1}. Chlorophyll *a* immediately decreased to a low level (<2 μg L^{-1}) following Storm C then increased to a peak value of >20 μg L^{-1} two weeks later. The subsequent tropical cyclone Cimaron and Jebi caused a smaller rainfall in the Jiulong River watershed, and salinity and nitrate changed little. Chlorophyll *a* dropped down again when cyclone Jebi landed. Peak chlorophyll *a* was observed with low turbidity and intermediate salinity (17–22 psu) towards the end of the sampling period (Fig. 6b, d). Chlorophyll *a* seemed to increase with water temperature but no significant correlation was found (Fig. 6e). There is no clear chlorophyll-nitrate relationship although higher chlorophyll *a* concentrates on the middle range of nitrate concentration (60–120 μmol L^{-1}) (Fig. 6c).

The cruise on July 24, 2013 (10 days after Storm C) down the entire estuary observed that NH_4-N and SRP were reduced in the Lower Estuary(Fig. 7). Moreover, the underway measurement captured several isolated peaks of chlorophyll *a* (>20 μg L^{-1}) there, compared with other waters (less than 10 μg L^{-1}). The high chlorophyll *a* values occurred at the same time as reduced NH_4-N and SRP. Based on molar C:N:P:Si ratios 106:16:1:20 (Conley et al., 1989; Redfield et al., 1963), these measurements shows that the Jiulong River Estuary and bay has nutrient fluxes much greater than 16 N:1P.

4. Discussion

4.1. Subdivisions of the estuary and the Estuary Turbidity Maximum

In this study, we divided the estuary into three parts. The Upper Estuary is the section from Station A4 to the location where the salinity begins to increase from 0.1 psu. This part of the estuary contains brackish water under normal flow conditions (Fig. 2). However, during storm flow the brackish water boundary moved downstream and this section of the estuary contains only freshwater with the increased nutrients and particulate matter (Fig. S3). It has flow characteristics similar to the river though modified somewhat by the wider channel characteristic of the estuary and much higher inferred flow than is present during normal flow conditions. As a result, it is suggested that it is subject to sediment scour and fine grained sediment deposited during normal flow conditions is liable to be resuspended during storms (Wengrove et al., 2015). Downstream is the Middle Estuary where the salinity increased from 0.1 to 5 psu. Within both the Upper and Middle Estuary there was a strong ETM, characterized by high SPM, which was present during major storms (C and D) but much reduced in the adjacent normal flow (Fig. 2). At other times, generally smaller turbidity maxima have been observed close to the 0–1 psu boundary (Dan Yu; unpublished data). ETM was reduced in case of small storm E. We hypothesize that because of the recurrent storms in the area, the fine sediment usually available for resuspension in a typical ETM has been scoured and transported downstream away from the Upper Estuary and is likely to take time to build up again. This is similar to the pattern suggested by Grabemann and Krause (2001) found in the Weser estuary. They found that during river floods the ETM is flushed towards the outer estuary and seemed to lose inventory of sediment and nutrients needing up to half a year of non-events to regain its former magnitude.

4.2. Effects of major storms on riverine inputs to the Upper Estuary

There was a major increase in both dissolved nutrients (N and P) and particulate matter brought down the river during major storms (Fig. S2 and Fig. 5) as has been observed in other river systems (Islam et al., 2016). In previous studies on the Jiulong River system, we demonstrated that such storms increase the riverine nutrient exports across the catchment but to different extents, depending on rainfall, antecedent soil moisture, and source supply (Chen et al., 2012). For the largest Storm C, the relatively lower NO_3-N concentration in the Upper Estuary compared with the other storms is probably due to strong dilution within the river channel by the high storm water (Fig. 3). By contrast for the more moderate Storm D with high antecedent soil moisture (large API) (Table 1), the higher nitrate concentration probably originated from redischarge of nitrate rich ground water (Chen et al., 2014a). During baseflow period, we have observed a high nitrate concentration (>480 μmol N L^{-1}) in the upstream of West River where land cash crops dominate (Chen et al., 2014a). Previous studies suggest that a large reservoir of nitrate in ground water may explain the mechanism of nitrate transfer from soil to stream when precipitation occur and groundwater level increase (Chen et al., 2012; Molenat et al., 2002) and is compatible with the observed delay in NO_3-N compared with the peak in the hydrograph (Fig. S2). Riverine ammonium was mainly from surface runoff particularly from over-land pollutants (e.g., sewage, manure) (Chen et al., 2012). NH_4-N concentrations were typically elevated at an early flood stage in all storm events (Fig. S2), which resulted in an enrichment of ammonium to the Upper Estuary in storm-affected periods (Fig. 3 and Table 2). Lower SRP concentrations in the river were observed in Storms C and D compared to Storm E (Table 2). This was ascribed to dilution of riverine SRP with rising water discharge, similar to previous storm data (Chen et al., 2015). Not surprisingly there was a large increase of TPP (and SPM) in riverine storm runoff since intensive rainfall usually causes soil erosion and large export of particulate P (Chen et al., 2015; Fraser et al., 1999; Nearing et al., 2004).

4.3. Effects of major storms on estuarine nutrient biogeochemical behaviors

In the Upper Estuary, there was an increase in NO_3-N (+90 μmol L^{-1} (Storm C), +163 μmol L^{-1} (Storm D) and +47 μmol L^{-1} (Storm E)), NH_4-N (+91 μmol L^{-1} (Storm C), +46 μmol L^{-1} (Storm D), +23 μmol L^{-1} (Storm E)), and SRP (+3.4 μmol L^{-1} (Storm C), +0.6 μmol L^{-1} (Storm D) and (+2.0 μmol L^{-1} (Storm E)) compared to the values in the river (Table 2). The probable cause for this major change in dissolved nutrient concentration was resuspension of sediment in the ~10 km of the Upper Estuary that is normally within the brackish section of the estuary but during major storms is scoured by the increased currents present within the river channel. Such sediment scour is a known characteristic of major storms (De Haas and Eisma, 1993; Lee et al., 2012; Wengrove et al., 2015). As this sediment is resuspended it includes both nutrient-rich pore waters, which adds to the nutrients measured in the overlying waters, and particulate matter.

A characteristic of such sediment in this part of the estuary is that it is generally high in organic carbon (9.56–16.6 mg kg^{-1}) and thus anoxic just below the sediment-water interface (SWI); Microelectrode DO profile reaches 0 μmol L^{-1} by 3–4 mm depth (Measured by E. Tan under 'normal conditions' in December 2015, unpubl.). Such pore waters characteristically have high concentrations of ammonium and SRP (Wengrove et al., 2015). Typically when such nutrient-rich sediments are advected into the overlying waters, ammonium and SRP are likely to rapidly desorb from particles (e.g. Froelich, 1988; Li et al., 2013; Percuoco et al., 2015). There was also an increase in nitrate in this part of the system as has been observed previously elsewhere (Zonta et al., 2005). In the Upper and Middle Estuary (A4, A5, A8), there was a large peak of nitrate (15–40 μmol L^{-1}) in sediments close to the SWI caused by in-situ nitrification (E. Tan unpubl.). Typically this suboxic

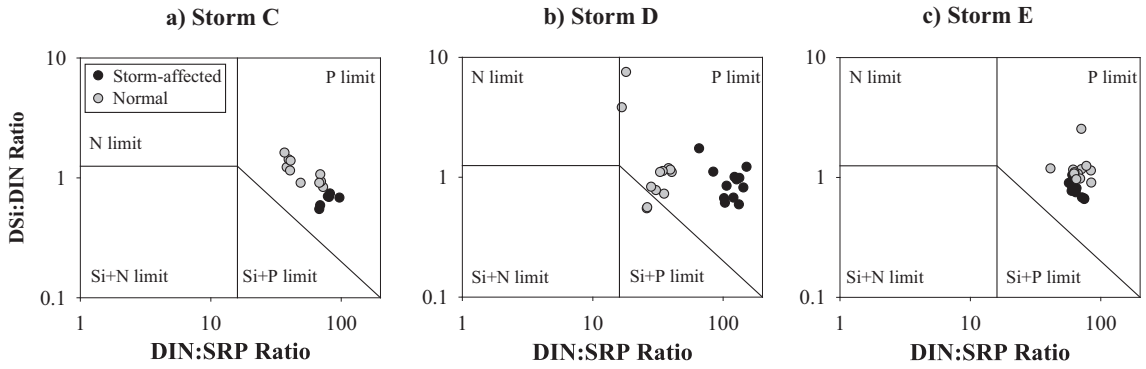

Fig. 4. Changes in N:P:Si ratios in storm affected conditions compared with normal flow conditions. Referenced lines indicates N:P:Si = 16:1:20 (molar ratio). Storm-affected refers to 1 day after storm C, 1 day after storm D and 1.4 days after storm E, respectively while normal condition refers to measured values 10 days after Storm C, 22 days after Storm D and 2.3 days before Storm E, respectively.

sediment is coated with nitrifying bacteria, which could also convert part of the dissolved ammonium into nitrate within the ETM (Schlarbaum et al., 2010). Together these processes could explain the increases in dissolved nitrate in the initial part of the ETM. While the diagenesis of organic matter in anoxic sediments is a relatively rapid process particularly in the relatively warm conditions of a subtropical estuary, the breakdown of silica is a slower process and hence the flux of DSi from resuspended sediment might be expected to be much smaller. The minor increase of DSi through REI to ECI supports this statement (Fig. 5). The resuspended sediment is likely to be dominantly the fine-grained sediment deposited in the Upper Estuary under normal flow conditions since the previous major storm. This would explain in part why the largest increases of SPM were observed in Storm C and D, while the increases in Storm E were much smaller. The smaller rainfall and river flow in Storm E also resulted in smaller increases in nutrient concentration.

An additional source of nutrients was external supply from surrounding runoff below ZS/JD (Eastern Zhangzhou urban and suburban area) and sediment resuspended from reservoirs immediately below the lowest river sampling stations. Our previous background

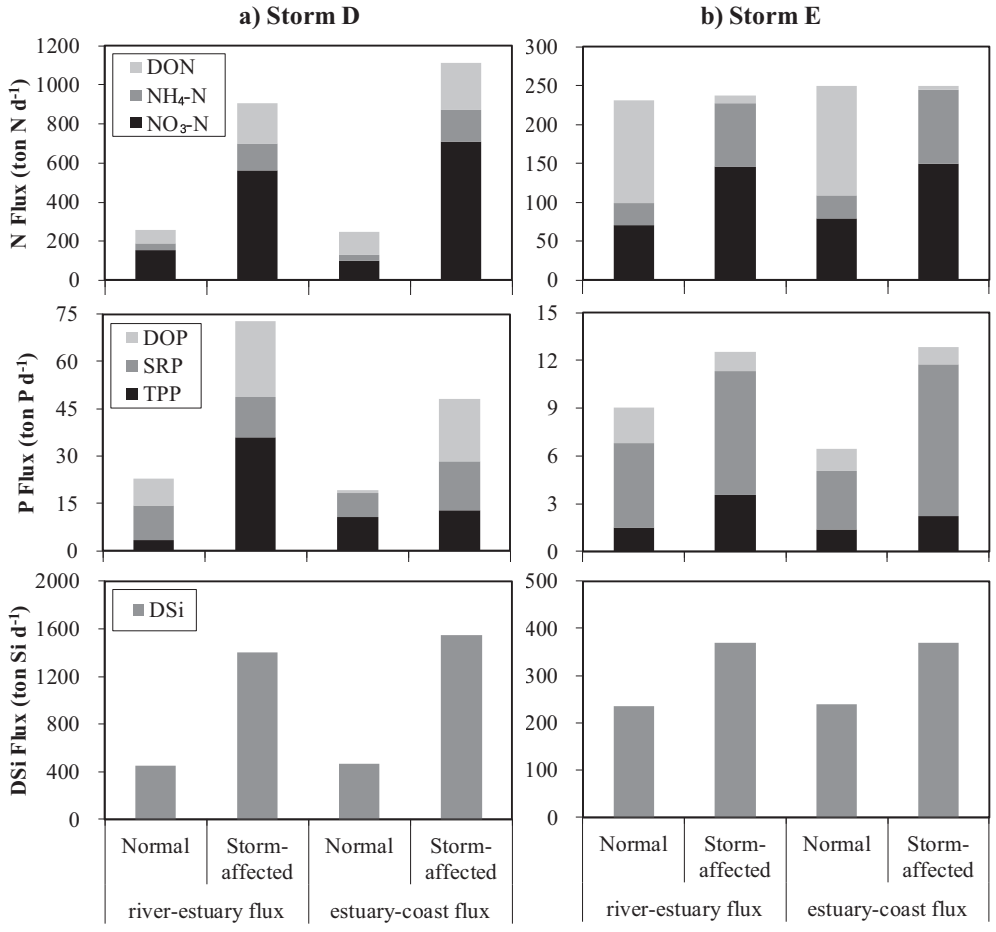

Fig. 5. Changes in nutrient fluxes across the river-estuary interface and the estuary-coast interface during Storm D and Storm E. Storm-affected refers to 1 day after Storm C, 1 day after Storm D and 1.4 days after Storm E, respectively while normal condition refers to measured values 10 days after Storm C, 22 days after Storm D and 2.3 days before Storm E, respectively.

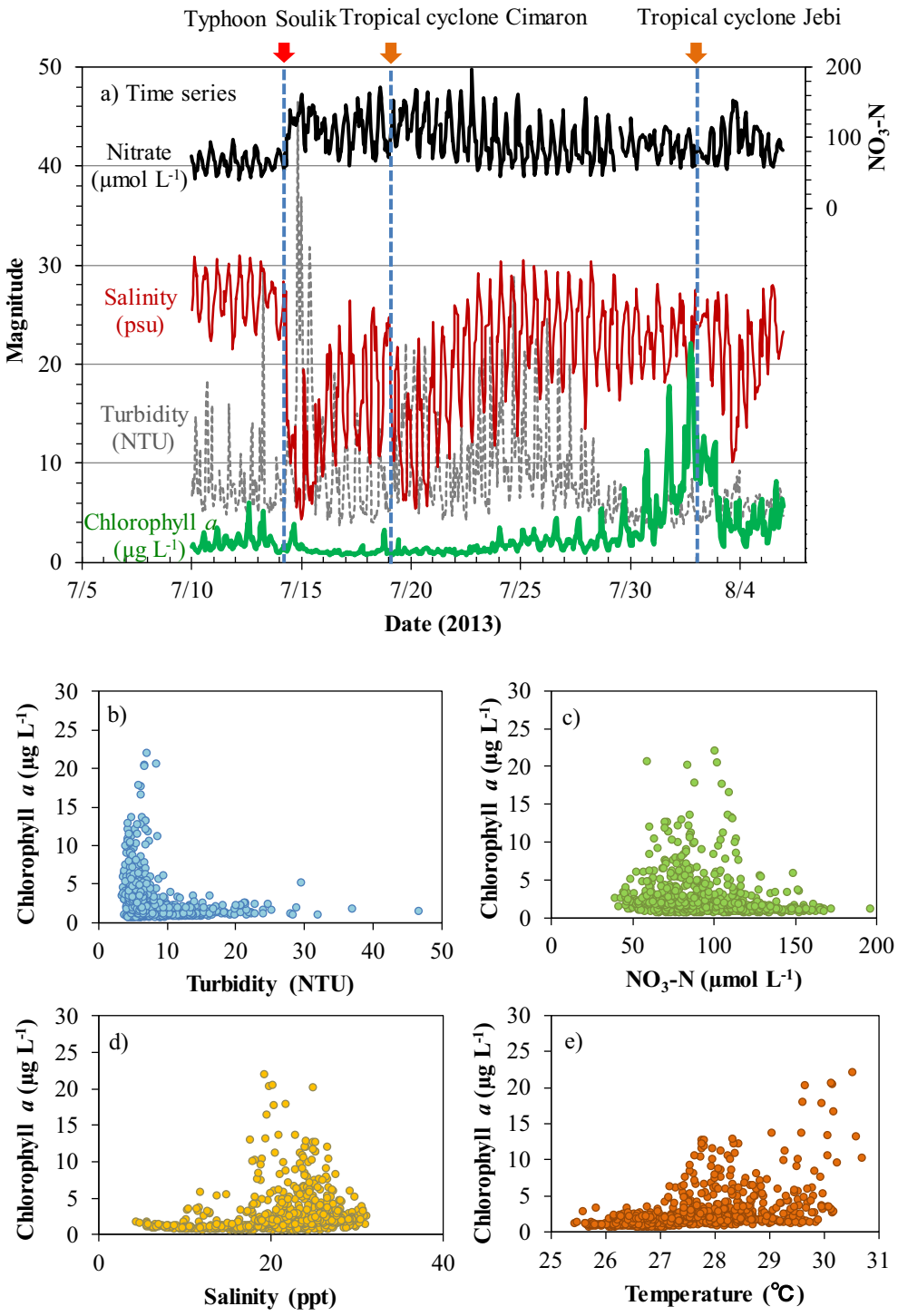

Fig. 6. Hourly variation of salinity, nitrate and chlorophyll in response to Storm C caused by typhoon Soulik, and two later rainfall events caused by tropical cyclone in July 2013 (a). Relationships between Chlorophyll *a* and turbidity (b), nitrate (c), salinity (d), and temperature (e). Data were obtained from the buoy (LOBO) deployed in Xiamen Bay (refer to Fig. 1).

measurement shows ammonium and nitrate concentration elevated in the lower West River (below ZS), ascribing to pollution discharge from urban and suburban area of Zhangzhou City (Chen et al., 2014a). The Beixi dike in the North river and the Xixi dike in the West river are located between the river stations (JD/ZS) and the Upper Estuary (A4). Under normal flow conditions, these are locations where sediment is trapped and dissolved nutrients reduced due to in-situ processes such as denitrification and biological uptake (Chen et al., 2014a; Wu et al., 2013). During storms the sluice gates are opened as a flood control measure and with the much increased flow and shorter water residence time it is likely not only will such removal processes be reduced but the previously deposited sediment could be resuspended. It is noted however that the SPM (and TPP) in the Upper Estuary was less than in the river at JD/ZS. We hypothesize that part of the flood induced SPM is deposited particularly when the flow rate decreases (falling limb of the hydrograph) and when storm runoff enter the wider river channel behind the dikes. This would result in the concentration of SPM and TPP reaching the Upper Estuary being somewhat lower than those measured in the river (Table 2). However it is a complex system. Further studies are needed to

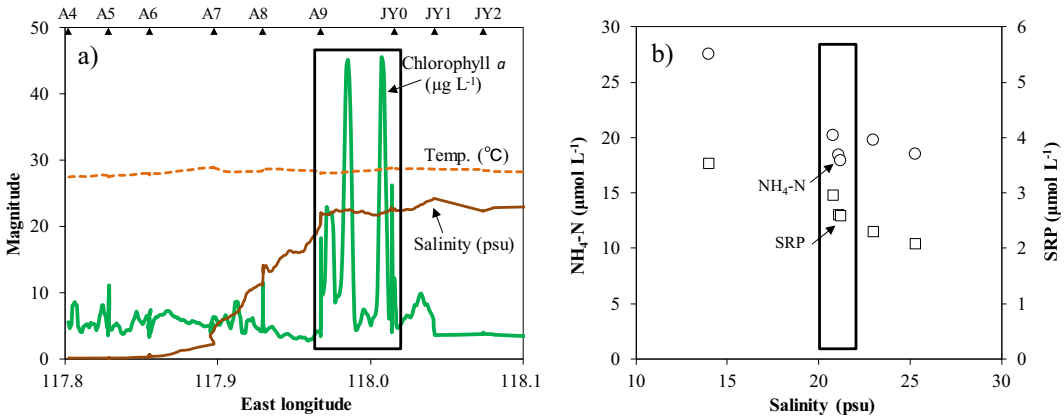

Fig. 7. Distribution of under way measurements (YSI) conducted 10 days (July 24, 2013) after Storm C that occurred on July 13, 2013 (a). The right panel (b) shows the removal of ammonium (circle) and phosphate (square) corresponding to the high chlorophyll *a* in the Lower Estuary (A9-JY0).

understand in more detail the balance of these processes between the reservoirs below the last sampling stations (ZS/JD) and in the Upper estuary (A4).

This explanation for within channel processes is consistent with the observation that the TDN and TDP fluxes through the estuarine-coastal interface (ECI) were greater than the fluxes through the river-estuary interface (REI) during major storm D (i.e. net export) and opposite to the pattern during normal flow of net deposition (Fig. 5). TPP accumulated in the estuary during the storms as SPM was deposited in the Middle and Lower Estuary.

Overall there was sharp increase in nutrient flux through both the REI interface and the ECI interface during the major Storm D compared with normal conditions (Fig. 5). N increased by a factor of >4 (REI) and >5 (ECI) while P increased by ~3.5 (REI) and >2 (ECI). By contrast there was relatively small increases of P and almost no increase in N at all in the small Storm E. Such increases in riverine nutrient fluxes caused by major storms have been seen previously (Chen et al., 2012; Chen et al., 2015). They represent an important fraction of the total transfer of bioavailable nutrients from lands into the coastal zone. The magnitude of the increased flux is a complex function of the magnitude of the storm, the previous history of storms in the catchment and recycling processes occurring in both the river and the estuary.

4.4. Ecological consequences of major storms in the Lower Estuary and coastal zone

The estuary and coastal ecosystem is sensitive to storm-driven pulse inputs of freshwater, particles and nutrients and associated changes in environmental condition (Bruesewitz et al., 2013; Paerl, 2006; Paerl et al., 2001). Our data, derived from a LOBO fixed station in the Xiamen Bay, showed an immediate decrease in chlorophyll *a* following Storm C (07/14/2013) which then increased to a peak value of >20 μg L^{-1} two weeks later (Fig. 6). Chlorophyll *a* was lowest with high turbidity (20–50 NTU) and peaked in the range of lower turbidity (<10 NTU). This suggests that high turbidity and light limitation was important factors in temporarily decreasing phytoplankton biomass (Shading effect). However, once the particulate matter settled out there were major peaks of chlorophyll *a* (up to 45.5 μg L^{-1}) in the Lower Estuary (Fig. 7). The highest chlorophyll *a* was found to coincide with middle salinity, nitrate, and higher temperature (Fig. 6c–e). The time-series data did not show a significant correlation between chlorophyll *a* and nitrate. As discussed above, the storms caused NH_4-N enrichment in the estuarine water. Although SRP was diluted just after Storm C it is likely to be replenished by desorption from particulate P (Fig. 3) due to the enhanced buffer effect (Froelich, 1988). Moreover, large particles (and organic matter) carried by storm runoff were deposited within the Middle and Lower Estuary. Subsequent mineralization would result in the release of ammonium and phosphate to the water column via pore water exchange (Ferguson et al., 2004; Hong et al., 2017). We inferred that ammonium and phosphate rather than nitrate act as the major nutrients supporting phytoplankton growth and bloom. This statement is supported by the observed removal of NH_4-N and SRP, accompanied by increased chlorophyll *a* at sampling sites in the Lower Estuary that were observed 10 days after Storm C (Fig. 7).

Major storms also substantially change the nutrient stoichiometry as well as total flux. The nature of nutrient cycling and flux varied however between storms and across the river-estuary-coast continuum (Fig. 5). In general, the fraction of DIN increased in storms while DON decreased. TDP dominated the total P, though TPP was relatively more important in storms particularly in the river and Upper Estuary. There was a minor increase in DSi fluxes during these storms as shown by the small increased flux between REI and ECI.

The N:P:Si ratio determines nutrient limitations that are important to regulating primary productivity and plankton communities in aquatic ecosystems (Domingues et al., 2005). River DSi was fairly high (246 ± 76 μmol L^{-1}) due to the granite lithology in the catchment and increased human perturbation and Si seems not to be a limiting nutrient in the Jiulong River (Chen et al., 2014b). The Jiulong River Estuary and bay is a potential P limited ecosystem according to their N:P:Si ratios (Fig. 4). The DIN:SRP ratios was high (29–68) and further increased during storm-affected periods. At the same time, the DSi:DIN decreased as a result of excess anthropogenic N loading over Silica (Chen et al., 2012; Chen et al., 2014b). Coastal eutrophication has been considered the consequence of unbalanced riverine nutrient inputs, with excess N and P over silica, compared to the requirements of the diatom growth (Billen and Garnier, 2007). Decreased DSi:DIN ratio was mainly correlated with agriculture (Downing et al., 2016). In North Carolina's Neuse R. Estuary (NRE), phytoplankton (chlorophyll *a*) responded to increased DIN:DIP ratio caused by hurricanes and tropical storms (Wetz and Paerl, 2008). Stormwater nutrient (high N:P ratio) inputs favor growth of non-native macroalgae (Rhodophyta) in the intertidal zone at O'ahu, Hawaiian Islands (Lapointe and Bedford, 2011). Although the phytoplankton assemblage was not determined in this study, previous studies have suggested that planktonic diatom community (e.g. *Skeletonema costatum*, and *Thalassiosira sp.*) predominate in both the Jiulong River Estuary and Xiamen Bay (Chen et al., 2009; Fu et al., 2016; Yan et al., 2015). In addition, if resting spores or resting cells of phytoplankton were present in the surface sediment, they would be re-suspended during storms into the water column. If the resting cells of fast glow phytoplankton were involved, then part of the rapid increase of chlorophyll *a* could have originated from these resting cells. However it is nonetheless likely that nutrient variation will have the greatest impact on phytoplankton evolution in Xiamen bay (Chen et al., 2010; Yan et al., 2015). Current results indicate that our estuary

and bay ecosystem tends to be more P limited following storms, and planktonic community might be sensitive and vulnerable to P loading and altered nutrient stoichiometry.

5. Conclusions

Storm-induced runoff increased the flux of nutrients into the Jiulong River Estuary, with the larger storms having the stronger effect. Given the interaction of rainfall, antecedent soil moisture, source supply and water flow in the river, the measured concentrations of nitrate, SRP and DSi could be diluted or enriched in storm runoff while ammonium concentration was generally elevated. Storm runoff carried a large amount of particles (SPM), resulting in a markedly increased concentration of TPP into the Jiulong River Estuary.

It was found that there was a storm induced ETM in the Upper and Middle Estuary (salinity <0.1–5 psu) that was not present during normal water flow. Here we defined the Upper Estuary as the part of the estuary that under normal flow conditions was the start of brackish water but during storms was freshwater because the fresh-saline water front moved approximately 10 km downstream during major storms. In this region of the estuary there was an increase in dissolved nutrients (NH_4-N, NO_3-N and SRP) compared with the concentrations measured in the river sampling stations. It was suggested that the dissolved nutrients came from river inflows with surrounding runoff, and resuspended sediment, which was scoured in the reservoirs behind the dikes and in the Upper Estuary. This increase was especially large in Storm D, which was the first major storm of the year and had sediment deposited for many months before the storm hit. Overall, more dissolved N and P were exported to the coast under major storm condition than were supplied through the REI while the opposite occurred during normal conditions.

There was increased chlorophyll *a* observed in Xiamen Bay as a result of the storm induced nutrient flux caused, once the SPM had been sedimented out and transparency increased. The changing nutrient supply and N:P:Si ratios during storms not only increased the potential for eutrophication in the Jiulong River Estuary and coastal zone but also increased the tendency towards P limitation in the receiving body of water. These results can be used to develop improved management practices in the river catchment and hence reduce eutrophication in the coastal waters.

Conflicts of interest

None.

Acknowledgements

This research was supported by the National Natural Science Foundation of China (No. 41376082; 41676098; U1305231), the Fundamental Research Funds for the Central Universities (20720160120), and the Program of Xiamen Southern Oceanographic Center (15PZB009NF05). We thank the crew on R/V Ocean II for their assistance in the cruises. We thank Ting Lu and all peoples who assisted in sampling and lab analysis. Special thanks are given to Hydrological Stations for providing hydrological data. We thank Professors R. Mortimer, Z. Chen, Y. Li and P. Cheng for their useful comments on this manuscript. We also wish to thank two anonymous reviewers for their very detailed and useful comments. This manuscript was written while MDK was a senior scientist at the Morris Kahn Marine Biological Station at Sdot Yam. This work was carried out as part of the GU-8 collaboration between Xiamen and Haifa Universities.

Appendix A. Supplementary data

Supplementary data to this article can be found online at https://doi.org/10.1016/j.scitotenv.2018.02.060.

References

Abril, G., Etcheber, H., Le Hir, P., Bassoullet, P., Boutier, B., Franki-Gnoulle, M., 1999. Oxic/anoxic oscillations and organic carbon mineralization in an estuarine maximum turbidity zone (The Gironde, France). Limnol. Oceanogr. 44, 1304–1315.
Biggs, R.B., Sharp, J.H., Church, T.M., Tramontano, J.M., 1983. Optical properties, suspended sediments, and chemistry associated with the turbidity maxima of the Delaware Estuary. Can. J. Fish. Aquat. Sci. 40, 172–179.
Billen, G., Garnier, J., 2007. River basin nutrient delivery to the coastal sea: assessing its potential to sustain new production of non-siliceous algae. Mar. Chem. 106, 148–160.
Bledsoe, E.L., Phlips, E.J., Jett, C.E., Donnelly, K.A., 2004. The relationships among phytoplankton biomass, nutrient loading and hydrodynamics in an inner-shelf estuary. Ophelia 58, 29–47.
Bruesewitz, D.A., Gardner, W.S., Mooney, R.F., Pollard, L., Buskey, E.J., 2013. Estuarine ecosystem function response to flood and drought in a shallow, semiarid estuary: nitrogen cycling and ecosystem metabolism. Limnol. Oceanogr. 58, 2293–2309.
Cao, W.Z., Hong, H.S., Yue, S.P., 2005. Modelling agricultural nitrogen contributions to the Jiulong River estuary and coastal water. Glob. Planet. Chang. 47, 111–121.
Chen, C.P., Sun, L., Gao, Y.H., Zhou, Q.Q., Zheng, M.H., Li, B.Q., Yu, Y., Lu, D.D., 2009. Seasonal changes of viable diatom resting stages in bottom sediments of Xiamen Bay, China. J. Sea Res. 61, 125–132.
Chen, B., Xu, Z., Zhou, Q., Chen, C., Gao, Y., Yang, S., Ji, W., 2010. Long-term changes of phytoplankton community in Xiagu waters of Xiamen, China. Acta Oceanol. Sin. 29, 104–114.
Chen, N., Wu, J., Hong, H., 2012. Effect of storm events on riverine nitrogen dynamics in a subtropical watershed, southeastern China. Sci. Total Environ. 431, 357–365.
Chen, N., Wu, J., Chen, Z., Lu, T., Wang, L., 2014a. Spatial-temporal variation of dissolved N2 and denitrification in an agricultural river network, southeast China. Agric. Ecosyst. Environ. 189, 1–10.
Chen, N., Wu, Y., Wu, J., Yan, X., Hong, H., 2014b. Natural and human influences on dissolved silica export from watershed to coast in Southeast China. J. Geophys. Res. Biogeosci. 119, 95–109.
Chen, N., Wu, Y., Chen, Z., Hong, H., 2015. Phosphorus export during storm events from a human perturbed watershed, southeast China: implications for coastal ecology. Estuar. Coast. Shelf Sci. 166, 178–188.
Cloern, J.E., 2001. Our evolving conceptual model of the coastal eutrophication problem. Mar. Ecol. Prog. Ser. 210, 223–253.
Conley, D.J., Kilham, S.S., Theriot, E., 1989. Differences in silica content between marine and freshwater diatoms. Limnol. Oceanogr. 34, 205–213.
Couceiro, F., Fones, G.R., Thompson, C.E., Statham, P.J., Sivyer, D.B., Parker, R., Kelly-Gerreyn, B.A., Amos, C.L., 2013. Impact of resuspension of cohesive sediments at the oyster grounds (North Sea) on nutrient exchange across the sediment–water interface. Biogeochemistry 113, 37–52.
De Haas, H., Eisma, D., 1993. Suspended-sediment transport in the Dollard estuary. Neth. J. Sea Res. 31, 37–42.
Dix, N., Phlips, E., Suscy, P., 2013. Factors controlling phytoplankton biomass in a subtropical coastal lagoon: relative scales of influence. Estuar. Coasts 36, 981–996.
Domingues, R.B., Barbosa, A., Galvao, H., 2005. Nutrients, light and phytoplankton succession in a temperate. Estuary (the Guadiana, south-western Iberia). Estuar. Coast. Shelf Sci. 64, 249–260.
Downing, J.A., Cherrier, C.T., Fulweiler, R.W., 2016. Low ratios of silica to dissolved nitrogen supplied to rivers arise from agriculture not reservoirs. Ecol. Lett. 19, 1414–1418.
Falkowski, P.G., Raven, J.A., 2013. Aquatic Photosynthesis. Princeton University Press, New Jersey.
Ferguson, A., Eyre, B., Gay, J., 2004. Nutrient cycling in the sub-tropical Brunswick estuary, Australia. Estuaries 27, 1–17.
Fraser, A., Harrod, T., Haygarth, P., 1999. The effect of rainfall intensity on soil erosion and particulate phosphorus transfer from arable soils. Water Sci. Technol. 39, 41–45.
Froelich, P.N., 1988. Kinetic control of dissolved phosphate in natural rivers and estuaries - a primer on the phosphate buffer mechanism. Limnol. Oceanogr. 33, 649–668.
Fu, T., Chen, B., Ji, W., Chen, H., Chen, W., Dong, X., Kuang, W., Chen, J., Wang, J., Lin, H., 2016. Size structure of phytoplankton community and its response to environmental factors in Xiamen Bay, China. Environ. Earth Sci. 75, 1–12.
Gobeil, C., Sundby, B., Silverberg, N., 1981. Factors influencing particulate matter geochemistry in the St. Lawrence estuary turbidity maximum. Mar. Chem. 10, 123–140.
Gong, G.C., Liu, K.K., Chiang, K.P., Hsiung, T.M., Chang, J., Chen, C.C., Hung, C.C., Chou, W.C., Chung, C.C., Chen, H.Y., Shiah, F.K., Tsai, A.Y., Hsieh, C.H., Shiao, J.C., Tseng, C.M., Hsu, S.C., Lee, H.J., Lee, M.A., Lin, I.I., Tsai, F.J., 2011. Yangtze River floods enhance coastal ocean phytoplankton biomass and potential fish production. Geophys. Res. Lett. 38.
Grabemann, I., Krause, G., 2001. On different time scales of suspended matter dynamics in the Weser estuary. Estuaries 24, 688–698.
Guo, W.D., Yang, L.Y., Hong, H.S., Stedmon, C.A., Wang, F.L., Xu, J., Xie, Y.Y., 2011. Assessing the dynamics of chromophoric dissolved organic matter in a subtropical estuary using parallel factor analysis. Mar. Chem. 124, 125–133.
Herbeck, L.S., Unger, D., Krumme, U., Liu, S.M., Jennerjahn, T.C., 2011. Typhoon-induced precipitation impact on nutrient and suspended matter dynamics of a tropical estuary affected by human activities in Hainan, China. Estuar. Coast. Shelf Sci. 93, 375–388.
Herman, P.M., Heip, C.H., 1999. Biogeochemistry of the MAximum TURbidity Zone of Estuaries (MATURE): some conclusions. J. Mar. Syst. 22, 89–104.
Hong, Q., Cai, P., Shi, X., Li, Q., Wang, G., 2017. Solute transport into the Jiulong River estuary via pore water exchange and submarine groundwater discharge: new insights from 224Ra/228Th disequilibrium. Geochim. Cosmochim. Acta 198, 338–359.
Islam, M.S., Bonner, J.S., Fuller, C.S., Kirkey, W., 2016. Impacts of an extreme weather-related episodic event on the Hudson river and estuary. Environ. Eng. Sci. 33, 270–282.

Lapointe, B.E., Bedford, B.J., 2011. Stormwater nutrient inputs favor growth of non-native macroalgae (Rhodophyta) on O'ahu, Hawaiian islands. Harmful Algae 10, 310–318.
Lee, J.H., Bang Jr., K.W., K., L.H., Choe, J.S., Yu, M.J., 2002. First flush analysis of urban storm runoff. Sci. Total Environ. 293, 163.
Lee, H.J., Park, J.Y., Lee, S.H., Lee, J.M., Kim, T.K., 2012. Suspended sediment transport in a rock-bound, macrotidal estuary: Han Estuary, Eastern Yellow Sea. J. Coast. Res. 29, 358–371.
Li, M., Whelan, M.J., Wang, G.Q., White, S.M., 2013. Phosphorus sorption and buffering mechanisms in suspended sediments from the Yangtze Estuary and Hangzhou Bay, China. Biogeosciences 10, 3341–3348.
Mackenzie, F.T., Ver, L.M., Lerman, A., 2002. Century-scale nitrogen and phosphorus controls of the carbon cycle. Chem. Geol. 190, 13–32.
McKee, L.J., Eyre, B.D., Hossain, S., 2000. Transport and retention of nitrogen and phosphorus in the sub-tropical Richmond River estuary, Australia - a budget approach. Biogeochemistry 50, 241–278.
Molenat, J., Durand, P., Gascuel-Odoux, C., Davy, P., Gruau, G., 2002. Mechanisms of nitrate transfer from soil to stream in an agricultural watershed of French Brittany. Water Air Soil Pollut. 133, 161–183.
Mortimer, R., Krom, M., Watson, P., Frickers, P., Davey, J., Clifton, R., 1999. Sediment–water exchange of nutrients in the intertidal zone of the Humber Estuary, UK. Mar. Pollut. Bull. 37, 261–279.
Nearing, M., Pruski, F., O'neal, M., 2004. Expected climate change impacts on soil erosion rates: a review. J. Soil Water Conserv. 59, 43–50.
Officer, C.B., 1979. Discussion of the behaviour of nonconservative dissolved constituents in estuaries. Estuar. Coast. Mar. Sci. 9, 91–94.
Paerl, H.W., 2006. Assessing and managing nutrient-enhanced eutrophication in estuarine and coastal waters: interactive effects of human and climatic perturbations. Ecol. Eng. 26, 40–54.
Paerl, H.W., Peierls, B.L., 2008. Ecological responses of the Neuse River-Pamlico sound estuarine continuum to a period of elevated hurricane activity: impacts of individual storms and longer-term trends. In: KD, McLaughlin (Ed.), Mitigating Impacts of Natural Hazards on Fishery Ecosystems. 64, pp. 101–116.
Paerl, H.W., Bales, J.D., Ausley, L.W., Buzzelli, C.P., Crowder, L.B., Eby, L.A., Fear, J.M., Go, M., Peierls, B.L., Richardson, T.L., 2001. Ecosystem impacts of three sequential hurricanes (Dennis, Floyd, and Irene) on the United States' largest lagoonal estuary, Pamlico Sound, NC. Proc. Natl. Acad. Sci. 98, 5655–5660.
Peierls, B.L., Christian, R.R., Paerl, H.W., 2003. Water quality and phytoplankton as indicators of hurricane impacts on a large estuarine ecosystem. Estuar. Coasts 26, 1329–1343.
Percuoco, V.P., Kalnejais, L.H., Officer, L.V., 2015. Nutrient release from the sediments of the Great Bay Estuary, N.H. USA. Estuar. Coast. Shelf Sci. 161, 76–87.
Perrone, J., Madramootoo, C.A., 1998. Improved curve number selection for runoff prediction. Can. J. Civ. Eng. 25, 728–734.
Qin, D., Manning, M., Chen, Z., Marquis, M., Averyt, K., Tignor, M., Miller, H., 2007. Climate change 2007: the physical science basis. Contribution of Working Group I to the Fourth Assessment Report of the Intergovernmental Panel on Climate Change. Cambridge University Press, Cambridge, UK, New York, NY, USA, p. 996.
Rabalais, N.N., Turner, R.E., Diaz, R.J., Justic, D., 2009. Global change and eutrophication of coastal waters. ICES J. Mar. Sci. 66, 1528–1537.
Rabalais, N., Diaz, R., Levin, L., Turner, R., Gilbert, D., Zhang, J., 2010. Dynamics and distribution of natural and human-caused hypoxia. Biogeosciences 7, 585–619.
Redfield, A.C., Ketchum, B.H., Richards, F.A., 1963. The influence of organisms on the composition of sea-water. In: Hill, M.N. (Ed.), The Sea. John Wiley, New York, pp. 12–37.
Schlarbaum, T., Daehnke, K., Emeis, K., 2010. Turnover of combined dissolved organic nitrogen and ammonium in the Elbe estuary/NW Europe: results of nitrogen isotope investigations. Mar. Chem. 119, 91–107.
Schubel, J., 1968. Turbidity maximum of the northern chesapeake bay. Science 161, 1013–1015.
Statham, P.J., 2012. Nutrients in estuaries - an overview and the potential impacts of climate change. Sci. Total Environ. 434, 213–227.
Vidon, P., Allan, C., Burns, D., Duval, T.P., Gurwick, N., Inamdar, S., Lowrance, R., Okay, J., Scott, D., Sebestyen, S., 2010. Hot spots and hot moments in riparian zones: potential for improved water quality management. J. Am. Water Resour. Assoc. 46, 278–298.
Wang, Y., Jiang, H., Jin, J.X., Zhang, X.Y., Lu, X.H., Wang, Y.Q., 2015. Spatial-temporal variations of chlorophyll-a in the adjacent aea area of the Yangtze River estuary influenced by Yangtze River discharge. Int. J. Environ. Res. Public Health 12, 5420–5438.
Wengrove, M.E., Foster, D.L., Kalnejais, L.H., Percuoco, V., Lippmann, T.C., 2015. Field and laboratory observations of bed stress and associated nutrient release in a tidal estuary. Estuar. Coast. Shelf Sci. 161, 11–24.
Wetz, M.S., Paerl, H.W., 2008. Estuarine phytoplankton responses to hurricanes and tropical storms with different characteristics (trajectory, rainfall, winds). Estuar. Coasts 31, 419–429.
Wu, J., Chen, N., Hong, H., Lu, T., Wang, L., Chen, Z., 2013. Direct measurement of dissolved N-2 and denitrification along a subtropical river-estuary gradient, China. Mar. Pollut. Bull. 66, 125–134.
Yan, X., Cai, R., Bai, Y., 2015. Long-term change of the marine environment and plankton in the Xiamen Sea under the influence of climate change and human sewage. Toxicol. Environ. Chem. Rev. 98, 669–678.
Zhang, J.-Z., Kelble, C.R., Fischer, C.J., Moore, L., 2009. Hurricane Katrina induced nutrient runoff from an agricultural area to coastal waters in Biscayne Bay, Florida. Estuar. Coast. Shelf Sci. 84, 209–218.
Zhou, W., Yin, K., Harrison, P.J., Lee, J.H.W., 2012. The influence of late summer typhoons and high river discharge on water quality in Hong Kong waters. Estuar. Coast. Shelf Sci. 111, 35–47.
Zonta, R., Collavini, F., Zaggia, L., Zuliani, A., 2005. The effect of floods on the transport of suspended sediments and contaminants: a case study from the estuary of the Dese River (Venice Lagoon, Italy). Environ. Int. 31, 948–958.